land

MDPI

Article

50-Year Urban Expansion Patterns in Shanghai: Analysis Using Impervious Surface Data and Simulation Models

Chen Gao [1,2], Yongjiu Feng [1,2,*], Rong Wang [1,2], Zhenkun Lei [1,2], Shurui Chen [1,2], Xiaoyan Tang [1,2] and Mengrong Xi [1,2]

[1] College of Surveying & Geo-Informatics, Tongji University, Shanghai 200092, China; 2110973@tongji.edu.cn (C.G.); 2210960@tongji.edu.cn (R.W.); zhenkun_lei@tongji.edu.cn (Z.L.); 2110969@tongji.edu.cn (S.C.); 2110970@tongji.edu.cn (X.T.); ximengrong@tongji.edu.cn (M.X.)
[2] The Shanghai Key Laboratory of Space Mapping and Remote Sensing for Planetary Exploration, Tongji University, Shanghai 200092, China
* Correspondence: yjfeng@tongji.edu.cn

Abstract: Megacities serve as crucial catalysts for national economic and social development, and Shanghai, one of China's most prominent metropolitan areas, exemplifies this transformative urbanization. To study Shanghai's urban expansion, we extracted urban land cover data from 1985 to 2020 using impervious area products and simulated urban expansion dynamics from 2021 to 2035 by employing the cellular automata model. Leveraging these data, we analyzed a 50-year period of urban expansion and investigated the drivers, including economic factors, population growth, and transportation infrastructure. Our findings indicate that the size of Shanghai's urban area in 2035 will be nearly 13 times that of 1985. Over these five decades, Shanghai's urban centroid shifted from the northeast to the southwest, with early urban expansion concentrated in the northeast and later expansion in the southwest. New urban patches primarily emerged at the edges of the initial urban area. As time progressed, areas with higher urban expansion intensity moved outward from the city center, mirroring the trend of urban expansion hotspots. Landscape indicators also demonstrated a trend of urban patches initially spreading and subsequently clustering. Overall, the development of Shanghai's metropolitan area exhibits substantial spatiotemporal heterogeneity. By integrating correlation analysis and generalized additive models, we quantified the impact of urban expansion drivers. The results show that economic and population factors had high correlation coefficients (over 0.97) with urban area, and proximity to the city center and road network greatly contributed to urban expansion. Our research amalgamates various theories and methods to analyze the spatiotemporal dynamics of urban expansion in metropolitan areas. This work provides a valuable data foundation to aid policymakers in designing effective metropolitan development policies.

Keywords: urban expansion; spatiotemporal dynamics; remote sensing monitoring; cellular automata

Citation: Gao, C.; Feng, Y.; Wang, R.; Lei, Z.; Chen, S.; Tang, X.; Xi, M. 50-Year Urban Expansion Patterns in Shanghai: Analysis Using Impervious Surface Data and Simulation Models. *Land* **2023**, *12*, 2065. https://doi.org/10.3390/land12112065

Academic Editors: Sergio Reyes and Federico B. Galacho-Jiménez

Received: 21 October 2023
Revised: 13 November 2023
Accepted: 14 November 2023
Published: 15 November 2023

1. Introduction

Over 50% of the global population now resides in cities, with 41% living in metropolitan areas, a number that is expected to steadily increase [1–3]. As global economies grow and urbanization accelerates, populations are increasingly concentrating in cities, particularly metropolitan areas. Thus, these areas have become focal points of continuing urbanization [4–6]. China is currently at a crucial phase of urbanization, with urban land continually expanding, especially in the Yangtze River Delta urban agglomeration [7,8]. Consequently, analyzing the dynamics and drivers of urban expansion in metropolitan areas is vital. Such analysis can provide essential data to support policymakers in urban planning [9–11].

Urban land expansion, an irreversible facet of urban development, inherently carries negative impacts spanning socioeconomic and environmental aspects [12,13]. Present challenges include the declining vitality of rural areas, property market bubbles, traffic

congestion, greenhouse gas emissions, and air pollution [14,15]. A particularly substantial impact is that urban land expansion encroaches on ecological lands, such as the forest and grassland, which are essential for maintaining the ecological balance and sustainable development of the region. This creates serious ecological and environmental concerns [16,17]. Thus, understanding the spatiotemporal patterns and dynamics of urban land expansion is critical. Such comprehension forms a theoretical foundation for optimizing the sustainable and high-quality development of metropolitan areas [18,19].

The study of urban morphology and expansion mechanisms has recently garnered attention in urban geography, focusing on both individual cities and urban agglomerations [10,20–22]. Earlier research relied on statistical data, remote sensing data, points of interest (POI), and spatiotemporal data from multi-platforms. These were integrated with geographical information systems (GISs) for spatial analysis, landscape ecology, and other methods to analyze and simulate urban expansion patterns [23,24]. Metropolitan areas, due to varying socioeconomic backgrounds and urbanization levels, exhibit differences in the spatiotemporal patterns and dynamic features of urban expansion [25]. This necessitates quantitative descriptions of urban expansion patterns and dynamics at different development stages for diverse metropolitan areas.

Shanghai emerged as the largest city in eastern China as early as the 1930s. Since then, it has maintained its robust development foundation, evolving into a world-recognized city and the commercial epicenter of China [26,27]. By 2020, Shanghai's total population exceeded 24.8 million, spanning an area of 6,340 square kilometers. Its unique developmental history has added to the complexity of Shanghai's urban spatial structure, making it a fascinating subject for a range of studies. Shanghai has become one of the most urbanized cities in China, as its urban population density, economic development, infrastructure construction, and public services are at the forefront of Chinese cities. Therefore, Shanghai's urban expansion process has garnered widespread academic interest [2,28,29]. Prior studies on Shanghai's urban expansion evolution and future patterns have typically relied on a limited number of remote sensing images with large time intervals [20,21]. This approach has resulted in a noticeable gap in the analysis of Shanghai's long-term expansion patterns and continuous time-interval dynamics [16,17].

As a hub of local and neighboring populations and economic activities, the Shanghai metropolitan area is affected by various factors, including economic development, population growth, and infrastructure conditions [30,31]. While the expansion of Shanghai's urban area and its increasing population have invigorated urban development, they have also intensified conflicts between human activities and land use [32,33]. As an important city in the Yangtze River Delta, Shanghai's challenges are more comprehensive and pronounced. Thus, identifying the drivers of Shanghai's urban expansion can offer valuable insights for other cities grappling with similar issues [34,35].

This study investigates the characteristics and drivers of urban expansion in metropolitan areas, using Shanghai as a case study. We selected impervious area products from 1985 to 2020 and extracted the city's built-up area using the threshold segmentation method. Subsequently, we simulated and forecasted urban expansion patterns for the period from 2021 to 2035. To analyze urban expansion dynamics, we utilized the centroid shift model, urban expansion intensity metrics, and landscape metrics. We combined these with spatial analysis methods to examine the patterns and dynamics of Shanghai's urban expansion from 1985 to 2035. Correlation coefficients and generalized additive models were employed to quantify the impact of urban expansion drivers. Our study seeks to enhance the methods of monitoring urban physical space and provide a valuable contribution towards sustainable development in Shanghai and other metropolitan areas.

2. Methods

2.1. Modelling Urban Expansion Pattern

Cellular automata (CA) are currently widely used to simulate urban dynamics. In our study, we implemented the CA model in UrbanCA [36] to simulate the urban expansion

dynamics of Shanghai from 2021 to 2035. The CA model incorporates the urban expansion drivers (P_{URD}), the neighborhood (P_{NEI}), the constraint factor (CF), and the random factor. In UrbanCA, the global transition probability (P_{GT}) of whether a cell transitions to an urban state at the next time point can be expressed as [36]:

$$P_{GT} = \frac{\left(P_{URD} \times (1 + S_{TIP})^{t-1} + P_{NEI} \times S_{LAP}\right) \times CF}{2} \quad (1)$$

where S_{TIP} represents a scaling parameter to adjust for probabilistic decay effects in the range 0.0–0.1, and S_{LAP} represents a scaling parameter to adjust for neighborhood effects in the range 0.5–1.0.

Incorporating logistic regression into the CA model, cells typically exhibit urban or non-urban states, with urbanization judged based on the values fetched at a given time. Based on logistic regression, the transition probability influenced by the driver can be expressed as [36,37]:

$$P_{URD} = \frac{e^{(a_0 + a_1 x_1 + \ldots + a_n x_n + by + \gamma)}}{1 + e^{(a_0 + a_1 x_1 + \ldots + a_n x_n + by + \gamma)}} \quad (2)$$

where a_0 denotes the constant, a_1–a_n denotes the weight of the independent variable x_1–x_n and $x_0 = 1$, b denotes the weight of the dependent variable y. Considering the socioeconomic and infrastructural factors for Shanghai's future development, we identified the distance to the administrative center and the distance to roads as the independent variables for the logistic regression.

2.2. Measuring Urban Expansion Scale

The urban expansion area (UEA) directly represents the change in the built-up land area over a specified period. On the other hand, the urban expansion speed (UES) indicates the average annual growth in the built-up land area over a certain time span. This metric takes into account the influence of the initial built-up land area on the change in expansion, thereby reflecting the rate of urban expansion per unit of time [27]. UEA (km^2) and UES (km^2/year) are used to monitor the urban physical space and can be expressed as:

$$\begin{cases} UEA = UA_{T+N} - UA_T \\ UES = \frac{UA_{T+N} - UA_T}{N} \end{cases} \quad (3)$$

where UA_{T+N} and UA_T are the areas of urban lands at time $T + N$ and T, respectively; N is the interval of the monitoring period (in years).

2.3. Measuring Urban Expansion Distribution

The centroid represents the average location of mass distribution. It is frequently used in studies of urban dynamics and land use type changes, as it can reflect the trajectory of regional urban expansion over time and space. In this study, we use the centroid coordinates to illustrate the pattern of centroid migration during Shanghai's urban expansion from 1985 to 2035. The centroid coordinates are calculated as [38]:

$$\begin{cases} X_N = \frac{\sum_{i=1}^{j} A_N \cdot X_i}{\sum_{i=1}^{j} A_N} \\ Y_N = \frac{\sum_{i=1}^{j} A_N \cdot Y_i}{\sum_{i=1}^{j} A_N} \\ Moving\ distance = \sqrt{(X_{N+T} - X_N)^2 + (Y_{N+T} - Y_N)^2} \end{cases} \quad (4)$$

where X_N and Y_N are the abscissa and ordinated of urban centroid in year N, respectively, A_N is the area of the ith urban land patch in year N, j is the total number of

urban land patches, and X_i and Y_i denote the abscissa and ordinate of the ith urban land patch, respectively.

2.4. Measuring Urban Expansion Intensity

Urban expansion intensity (UEI) represents the percentage of the urban land expansion area of a spatial unit over the total area in a unit of time [39]. It is used to analyze the current status of urban expansion and to compare the intensity, speed, and trend of urban expansion in different directions. The expression is [40]:

$$UEI = \frac{UEA_N}{Unit \cdot N} \times 100\% \quad (5)$$

where UEA_N is the increased urban area in the study interval, and the $Unit$ is usually a 1 km × 1 km square grid.

To further elucidate the spatial changes associated with urban expansion, we established 22 circular buffer zones with a radius of 2 km, using the 1985 centroid of Shanghai as the origin. The above buffer radius leads to an appropriate number of buffers in the Shanghai region and these buffers cover the entire study area, which in turn provides sufficient sampling data for the urban expansion gradient analysis. Through spatial overlapping and GIS spatial analysis, we calculated the UEA within each buffer zone and examined the relationship between the UEA and the distance to the city center at different times [41,42]. Identifying the location and changes in areas of substantial urban expansion (hotspots) is crucial for urban planning and decision-making processes [41,43].

2.5. Measuring Urban Expansion Structure

Landscape metrics are commonly deployed to quantify variances in the form and structure of the physical space of urban landscapes. These metrics facilitate the analysis of patch shape, size, and dominance from multiple perspectives [44]. Due to the correlation between the landscape metrics, six commonly used class-level landscape metrics were selected for this study to comprehensively reflect the urban landscape pattern (Table 1). Patterns and processes of change in urban landscapes were described and quantified using the FRAGSTATS 4.2 software. It is important to note that all metrics are calculated exclusively for urban categories [45].

Table 1. The landscape metrics applied to assess urban land pattern.

Category	Name	Description
Area edge	Percentage of landscape (PLAND)	The percent of the study area comprised of different land use types
	Edge density (ED)	The ratio of land use patch perimeters to its areas
Shape	Perimeter-area fractal dimension (PAFRAC)	The relationship between perimeter and area to reflect shape complexity
	Mean patch shape index (SHAPE_MN)	The average complexity of the patch shape in the study area
Aggregation	Largest patch index (LPI)	The percentage of the largest patch in the total landscape area
	Landscape shape index (LSI)	Total edge length adjusted by the study area size

2.6. Quantifing Urban Expansion Drivers

Correlation analysis is a statistical method used to evaluate the degree of association between two independent variables. It measures if and how strongly the two variables are related [46]. To more accurately measure the strength of the relationship between Shanghai's urban expansion and its drivers, we utilized the correlation coefficient. The Pearson correlation coefficient is frequently used to analyze the degree of association

between variables. Its value ranges from −1 to 1. A negative value indicates a negative correlation, while a positive value indicates a positive correlation [47].

Buffer analysis is a key function of spatial analysis in GIS. It creates a region, or a polygon layer, at a specified distance around the boundary of a geographic element to identify its area of influence [48]. In this study, we used buffer analysis to extract urban expansion at different distances from various types of roads. This approach was designed to reflect the role of the transport network in driving urban expansion.

A generalized additive model (GAM) transforms nonlinear dependent and independent variables into a linear relationship [49]. In this study, the GAM is used to examine the quantitative relationship between urban expansion and its drivers. This is accomplished by associating Shanghai's historical urban expansion with its drivers through a smoothing function, creating an individual model, and then sequentially incorporating the drivers into the GAM model based on their explanatory power.

3. Study Area and Data Sources

3.1. Study Area

Situated at the mouth of the Yangtze and Huangpu rivers in eastern China, Shanghai is one of the country's largest world cities. It spans a total area of 6340.5 square kilometers and boasted a population exceeding 24 million in 2015. The city encompasses 16 districts, 7 of which are central districts: Huangpu, Xuhui, Changning, Jing'an, Putuo, Hongkou, and Yangpu (Figure 1). Since 1985, Shanghai has undergone a substantial transition from rural to urban, propelled by rapid urbanization. This process has seen the city expand into peripheral suburbs, often at the cost of valuable agricultural land. Over the past three decades, the Shanghai metropolitan area has experienced swift urban expansion accompanied by dramatic demographic and economic shifts [34]. This substantial urban expansion has led to serious ecological degradation, environmental pollution, and the onset of other "urban diseases", such as the deterioration of urban air and water quality. These issues pose severe challenges for local policy makers [50,51]. Therefore, it is essential to explore the spatial and temporal patterns and dynamics of urban expansion in the Shanghai metropolitan area.

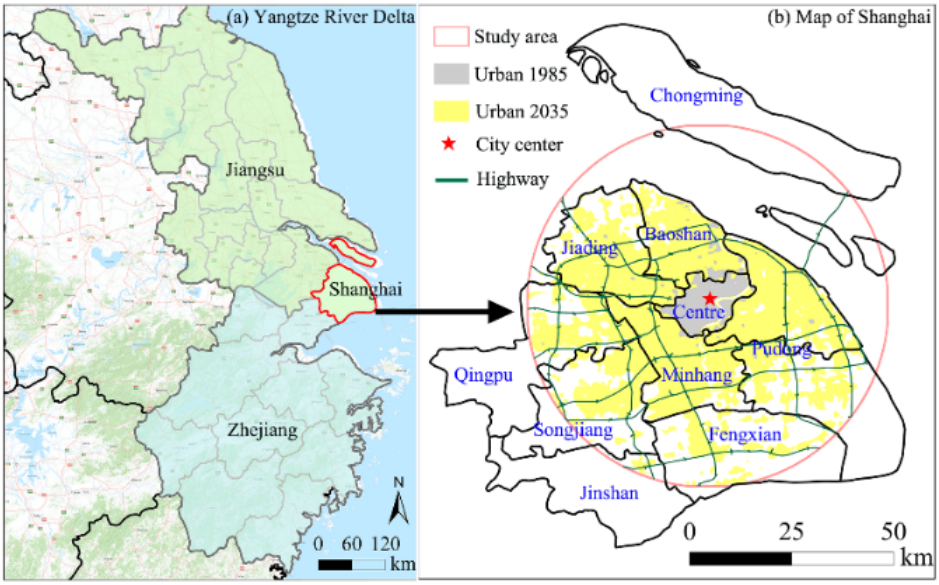

Figure 1. The Shanghai study area: (**a**) Yangtze River Delta urban agglomeration and (**b**) Shanghai city.

3.2. Data Source

In this study, the urban land use map of Shanghai was derived from existing impervious surface products. The data spanning from 1985 to 2018 were provided by Gong, Li [52], while the data for 2019 and 2020 came from Zhang, Liu [53]. The data from 1985 to 2018

were mapped impervious surfaces with a 30 m resolution using reliable impervious surface mapping algorithms and the Google Earth Engine (GEE) platform. The 2019 and 2020 data were acquired through impervious surface extraction algorithms based on multi-source, multi-temporal remote sensing data. These datasets have undergone cross-validation and comparative analysis, ensuring high accuracy. Given their extensive time series, continuous growth patterns, and spatiotemporal dynamics of land use, these are the most suitable maps of Shanghai for analyzing the city's development and growth process.

All socioeconomic data (including GDP and population) for Shanghai from 1985 to 2020 were sourced from the Shanghai Municipal Bureau of Statistics. Vector-based maps were utilized to delineate administrative boundaries and to generate spatial factors influencing urban expansion, as indicated in Table 2. The administrative map, used to define administrative boundaries and the city center of Shanghai, was obtained from the Geographical Information Monitoring Cloud Platform (www.dsac.cn; accessed on 15 June 2021). Road network maps, defining primary roads, highways, railway lines, and subways, were sourced from OpenStreetMap (www.openstreetmap.org). These road network maps were utilized to extract proximity factors that impact urban expansion, such as distance to primary roads, highways, railway lines, and subway routes.

Table 2. Vector datasets for urban expansion analysis.

Datasets	Source	Scale	Used to
Administrative map	Geographical Information Monitoring Cloud Platform	1:1,000,000	Extract boundary and administration centers
Road network map	OpenStreetMap	1:1000	Extract primary roads, highways, and railways
Subway networks	OpenStreetMap	1:1000	Extract subway lines

4. Results

4.1. Urban Patterns and Expansion 1985–2035

Utilizing impervious surface products as foundational data, we employed a threshold division to categorize land areas with built-up intensity exceeding 0.5 as urban land. Initially, we procured data pertaining to urban land in Shanghai from 1985 through 2020. Subsequently, we calibrated the CA model by simulating Shanghai's urban expansion from 2000 to 2010 and validated the CA model using the actual urban layout of Shanghai from 2010 to 2020. The overall accuracy for the years 2010 and 2020 was 83.6% and 89.4%, respectively, while the figure of merit for the same years was 40.2% and 39.8%, respectively. These results affirmed the reliability of the CA model. Using the 2020 urban layout of Shanghai as the initial state, we projected the urban pattern for the period 2021–2035.

From 1985 to 2035, the majority of Shanghai's urban expansion manifests as edge-type growth, primarily along the initial urban fringe of the central city (Figure 2). Urban expansion in Shanghai from 1985 to 1995 was principally concentrated in the city center, with less growth occurring outside this area, and a pattern of outward expansion and inward infill predominating. In the period from 1995 to 2005, urban growth around the city center was largely characterized by fringe and infill expansion, while expansion in the areas surrounding the city center and in the suburbs primarily took the form of growth along the initial urban fringe. The decade from 2005 to 2015 witnessed the most intense period of urban expansion in the entire span studied, with more infill expansion occurring in the city center than on the fringe. The city center was nearly entirely urban land during this period, and outward expansion virtually came to a halt. Concurrently, urban expansion in areas adjacent to the city center gradually decreased, whereas urban expansion outside these areas was more pronounced. The simulations show that there is no further urban expansion in and around the city center, while suburban expansion is no longer pronounced from 2015 to 2035.

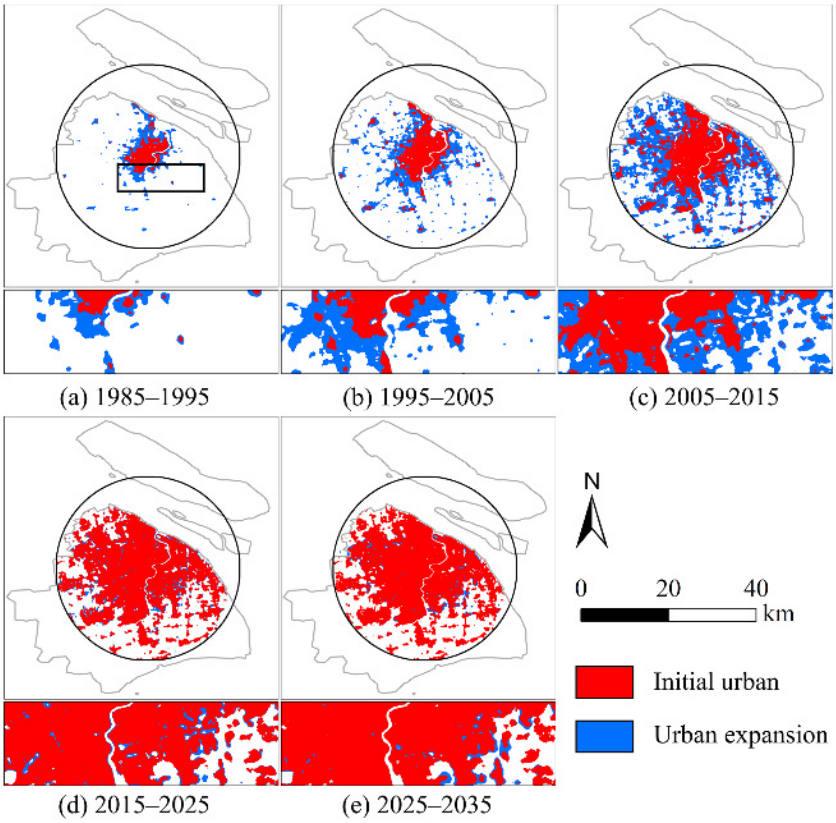

Figure 2. Urban expansion patterns and dynamics in Shanghai 1985–2035 (10-year interval).

4.2. Annual Urban Expansion

4.2.1. The Size and Rate of Urban Expansion

The urban expanse of Shanghai has consistently expanded from 179.5 km^2 in 1985 to 2343.8 km^2 in 2035, marking an increase of nearly 13-fold (Figure 3a). The rate of urban expansion across each observation period has been uneven, with a continuous deceleration in the pace of urban growth across each observation period from 1985 to 1989 (Figure 3b). In the period from 1989 to 1990, the pace of urban expansion surged to approximately 26 km^2 per year. By 1991, the rate of urban expansion exhibited a declining trend, while the speed of Shanghai's urban expansion presented an upward trend in each of the monitoring periods from 1991 to 1994. Starting from 1995, the speed of urban expansion in Shanghai has demonstrated a substantial upward trend. Subsequently, this consistently increasing pace of urban expansion decelerates until 2013. By 2020, the rate of urban expansion stabilizes at 10 km^2 per year; by 2035, the pace of Shanghai's urban expansion has leveled off, suggesting that the city center area is nearing saturation in terms of the amount of land that can be transformed into urban land.

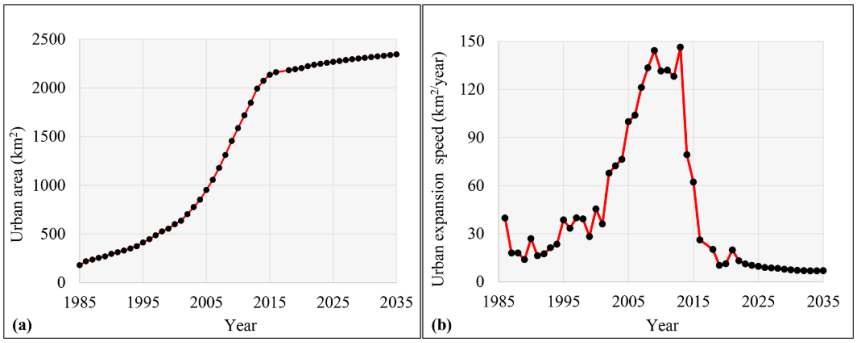

Figure 3. Urban expansion scales for Shanghai, 1985–2035: (**a**) The total urban area and (**b**) UES per year.

The location of the centroid in Shanghai is continually shifting, with the focal point of the entire urban area's expansion moving predominantly towards the southwest (as shown in Figure 4). From 1985 to 1990, the centroid exhibited a westward trend, with the most substantial shift occurring between 1985 and 1986 and the least substantial between 1987 and 1988. After 1990, the centroid transitioned from a westward to a southwestern direction. From 1999 to 2000, the centroid slightly shifted to the southeast, and the shift of the centroid from 2000 to 2006 was the most pronounced over 50 years, especially in the observation periods of 2003–2004, 2004–2005, and 2005–2006. Since 2010, the centroid has persistently moved southwards, has moved westwards sporadically, and, at times, has displayed a tendency to shift eastwards. The location of the centroid changes minimally after 2015, particularly from 2020 to 2035, during which the centroid barely moves. The movement direction of the centroid reflects the principal trend of urban expansion, indicating that the urban areas have transitioned from the northeast to the southwest.

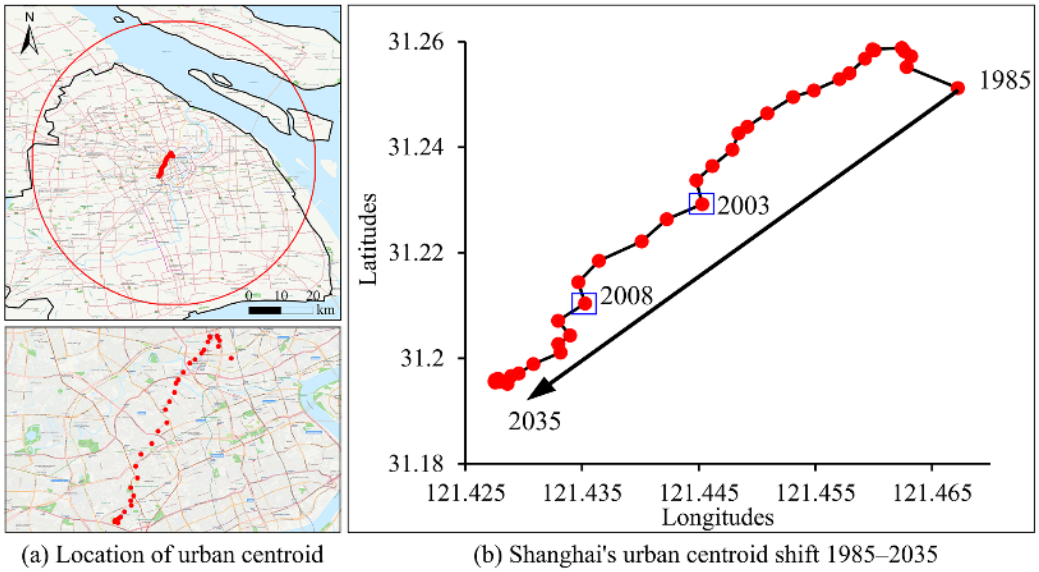

(a) Location of urban centroid (b) Shanghai's urban centroid shift 1985–2035

Figure 4. Urban centroid locations and its moving detail from 1985 to 2035.

4.2.2. The Intensity and Structure of Urban Expansion

The average urban expansion intensity within the circular buffer zone was analyzed using the city center of Shanghai in 1985 as the circular point. The results reveal that from 1985 to 2000, the peak intensity of urban expansion in Shanghai occurred within a 20 km radius of Shanghai's city center and was mainly concentrated at distances of 8–14 km (as shown in Figure 5). For example, the urban expansion intensity reached a maximum at the 8 km mark in 1985–1986, indicating that urban expansion occurred primarily in the immediate vicinity of the initial urban area. After 2000, the intensity of urban expansion substantially increased beyond the 20 km mark within the buffer zone. During the period from 2000 to 2020, the intensity of urban expansion in built-up areas exhibited a trend of increasing and then decreasing over time. Beyond 2020, the average urban expansion intensity within each buffer ring is less than 2%, with the peak occurring in the area located 22 km from the city center.

We utilized landscape metrics to analyze the spatial structure of Shanghai's urban expansion over 50 years (as illustrated in Figure 6). Between 1985 and 2035, the total edge of the city decreased as the urban area increased, which aligns with the infill development revealed by the PLAND and LPI metrics. From 1985 to 2035, PLAND increased from 3.46 to 45.18 and LPI escalated from 2.81 to 40.71. The two area-edge metrics surged rapidly in the early phase, and the growth rate decelerated substantially in the later phase. As the size of urban areas expands, the edge density of urban patches substantially increases, and the increase in ED diminishes from 1985 to 2020, with a downward trend in the subsequent

years: ED was 0.57 in 1985, rose to 5.84 in 2020, and then dropped to 4.28 in 2035. The SHAPE_MN in Shanghai has oscillated between 1.2 and 1.4 over 50 years, reaching a peak of 1.39 in 2007. The decrease in the PAFRAC metric reflects the diminishing shape complexity of the urban patches in the later stage, which displays similar implications to the LSI metric. LSI continued to rise until 2020, and a downward trend was predicted from 2021 onwards. All landscape metrics indicate that Shanghai's urban expansion combines a diffusion effect, expanding the city's external boundaries, and a clustering effect, filling in non-urban areas and thus connecting adjacent urban areas.

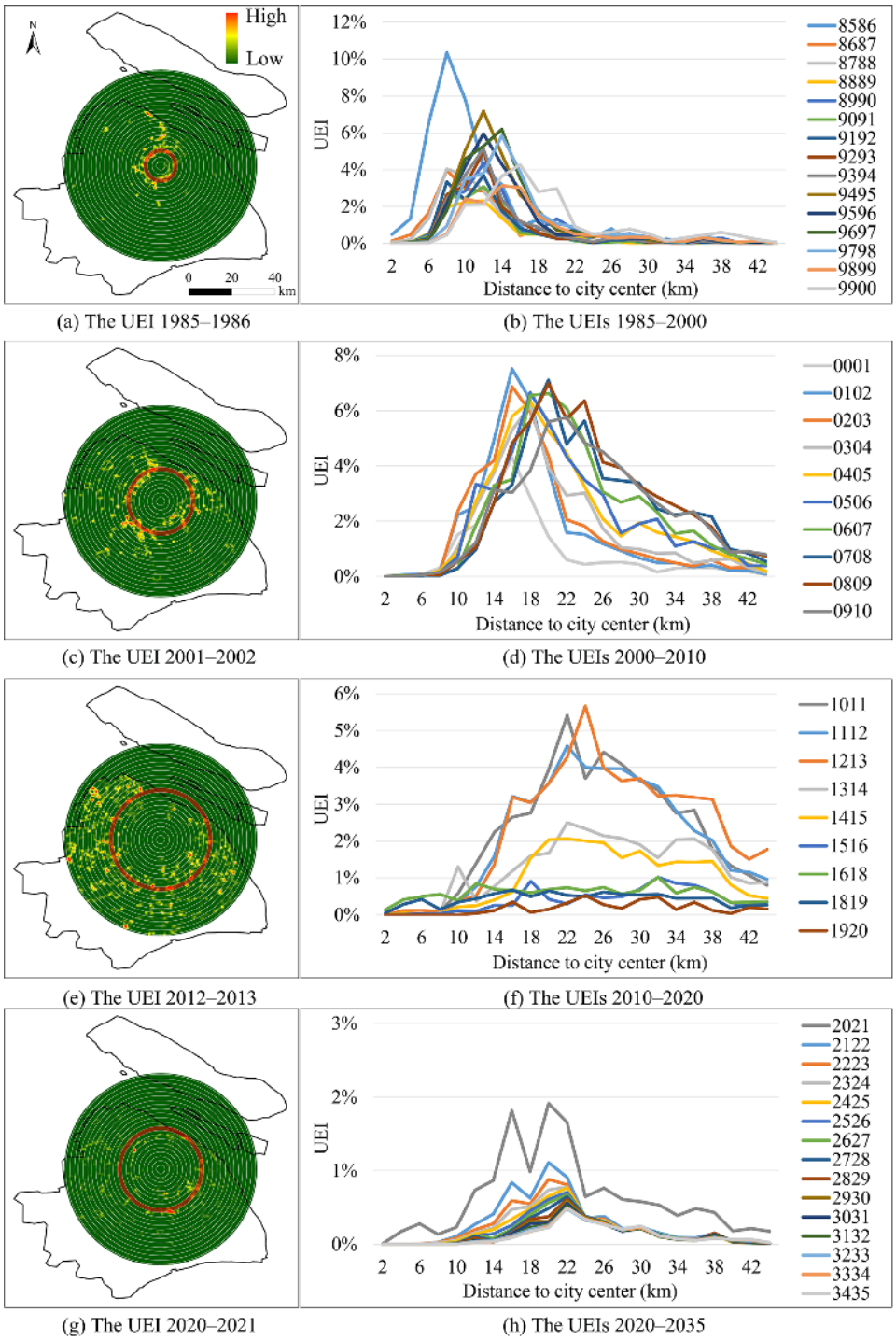

Figure 5. Urban expansion intensity 1985–2035 and the year containing the most dramatic UEI in each time period (The red circle in the left column is the area with the largest UEI).

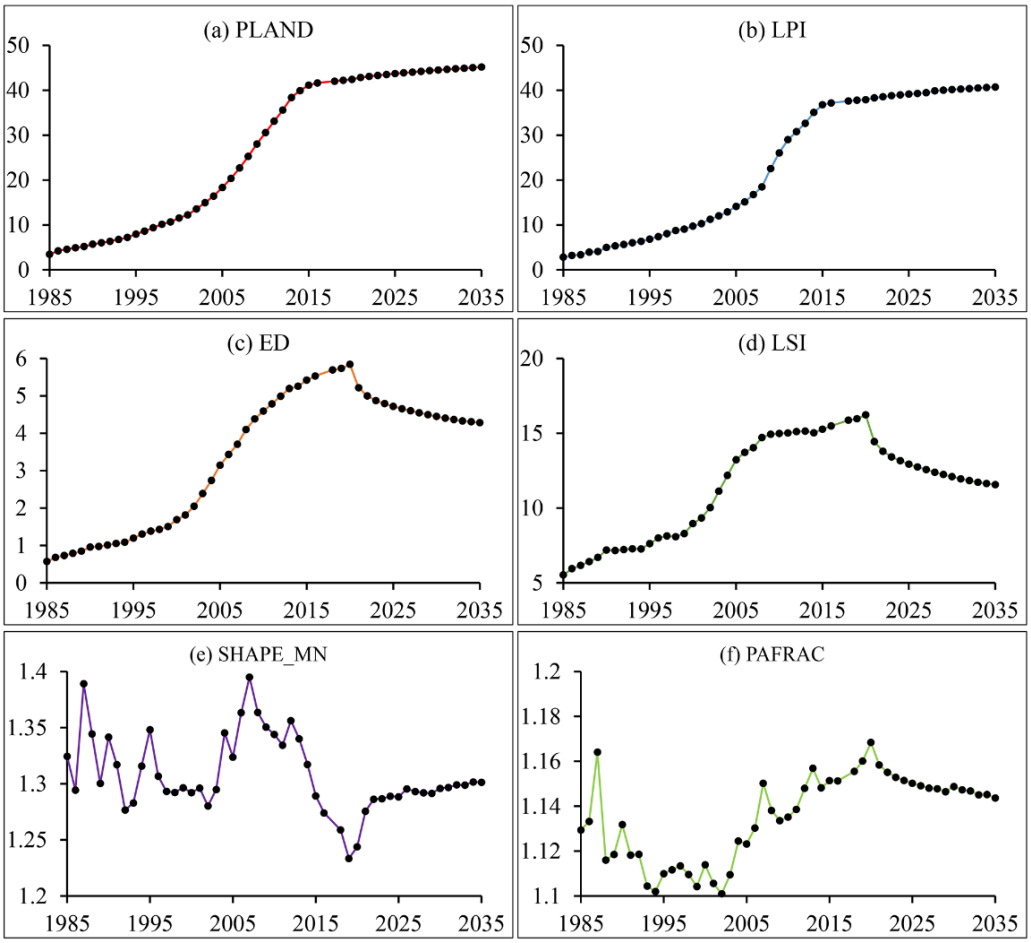

Figure 6. Landscape metrics of urban during 1985–2035 (horizontal coordinates are years).

4.3. Five-Year Interval of Urban Expansion

4.3.1. Gradient-Based Spatial Heterogeneity Analysis

Analyzing the gradient changes of hotspots in Shanghai's urban expansion over 50 years can shed light on the spatial heterogeneity of its expansion (as depicted in Figure 7). Between 1985 and 2000, the hotspots of urban area growth primarily occurred at distances of 8–10 km, 10–12 km, and 12–14 km, indicating substantial urban expansion in areas closer to the city center. Beyond 2000, the hotspots clearly shifted outwards, concentrated at distances of 16–18 km and 18–20 km. This suggests that there are almost no more areas within 16 km from the city center available for urban land expansion. However, from 2010 to 2020, there is little difference in UEAs beyond 22 km from the city center, with no more prominent hotspots of urban expansion. The simulation results for 2020–2035 show hotspots of urban expansion within the 20–22 km range. Compared to the previous period, the trend of urban migration is not apparent. Notably, after 2000, all of Shanghai's urban expansion hotspots are located beyond 16 km.

4.3.2. Direction-Based Spatial Heterogeneity Analysis

Using the city center as the center of the circle, we divided the study area into eight sectors and tallied the area of urban expansion in each sector's direction to further probe the spatial heterogeneity of urban expansion (Figure 8). From 1985 to 2000, there was less urban expansion in the eastern region, especially in the southeastern region, where the expansion was the smallest. Expansion was relatively balanced in all directions except in the north, where the area of urban expansion was larger. The trend of urban expansion in the different directions during 2000–2010 is quite distinct from the previous period. The area of urban expansion in the north has substantially decreased. With the exception of the

north and northeast, the trend of urban expansion in area is substantial in other directions. During the period 2010–2020, urban expansion is concentrated in the northwest, west, southwest, south, and southeast of the study area, with urban expansion less pronounced in the east than it was 10 years prior. From 2020 to 2035, urban expansion cells will mainly occur in the southeastern part of Shanghai, with smaller urban expansion in the north and larger urban expansion in the west. Overall, the UEA in all directions in recent years and in the future does not increase over time, but rather shows a decreasing trend. Early urban expansion was evident in the northern region, and subsequent urban expansion cells are mainly located in the southern part of the study area.

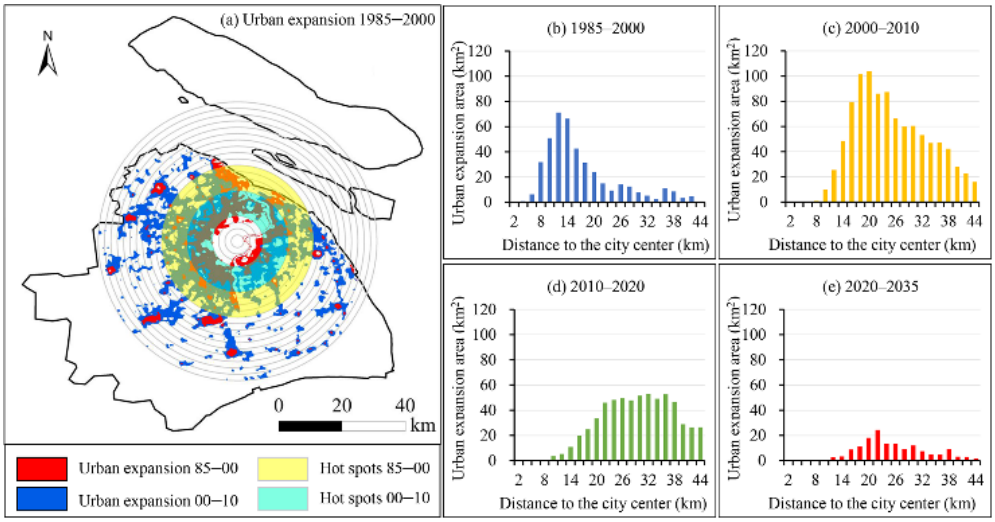

Figure 7. Gradient changes in urban expansion and the location of hotspots.

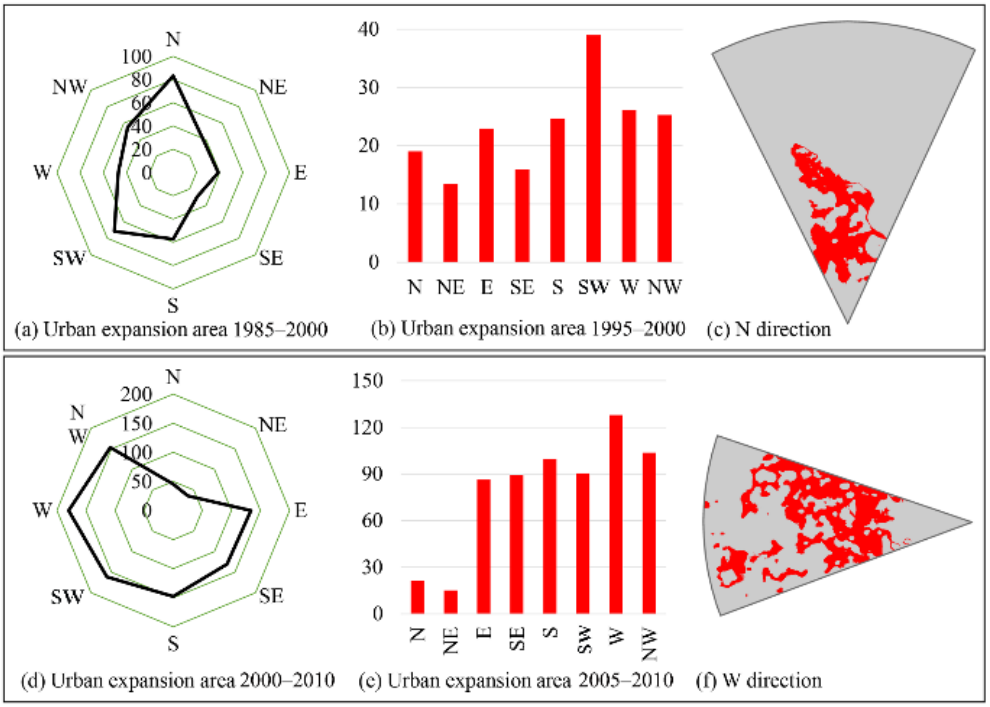

Figure 8. *Cont.*

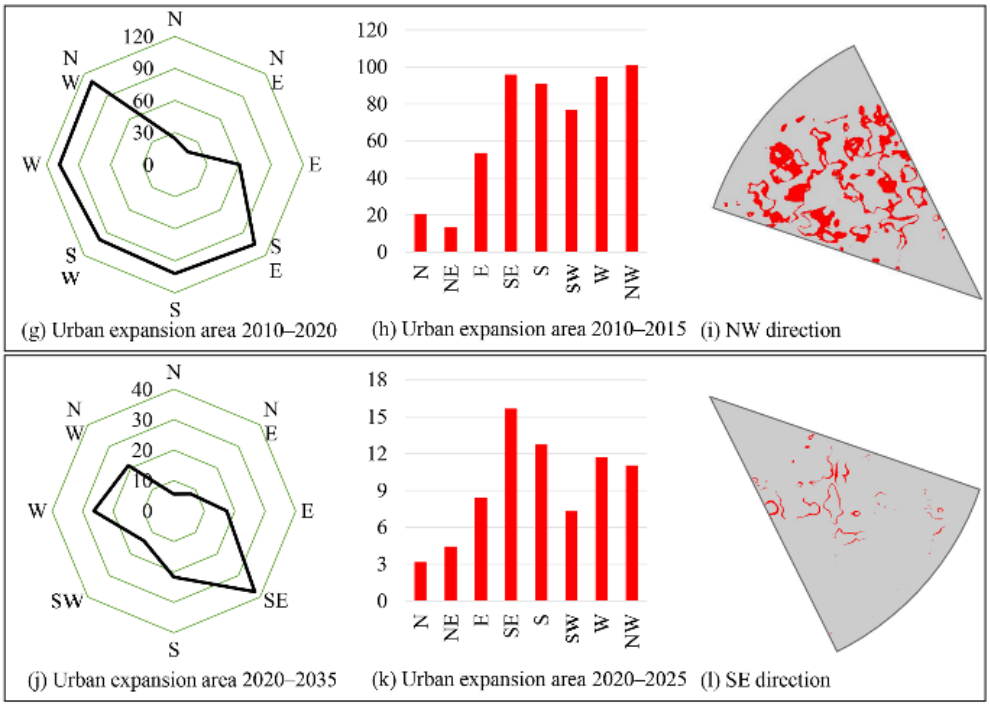

Figure 8. Expansion of urban land area in eight different directions: left column shows UEAs at 10- or 15-year intervals; center column shows the 5 years with the most UEAs during the 10- or 15-year intervals; and right column shows the direction with the most UEAs during the 5-year interval.

4.4. Urban Expansion Drivers 1985–2020

4.4.1. The Socioeconomic Effects on Urban Expansion

Population is the most dynamic component of a megalopolis. Shanghai's population has shown an overall trend of continuous growth, increasing from 12.33 million to 24.88 million from 1985 to 2020 (as shown in Figure 9). Statistically, the primary source of Shanghai's population growth is mainly attributed to the mass influx of rural people into the city. Simultaneously, the improvement in living standards has led to higher requirements for housing quality, accelerating the process of property development and driving the city's continuous expansion. There is a highly linear relationship between Shanghai's total population and its urban area, with an R^2 value exceeding 0.97; the correlation coefficient between the two is also above 0.98 (as shown in Table 3), indicating a similar trend. Hence, the increase in urban population can be identified as one of the most critical factors influencing the dynamics of Shanghai's urban expansion from 1985 to 2020.

Table 3. Correlation of urban area with socioeconomic factors.

Category	UA vs. POP	UA vs. GDP	UEA vs. POP	UEA vs. GDP
Pearson correlation	0.987	0.976	0.472	0.172
Significance	0.01	0.01	0.004	0.323
N	36	36	35	35

Economic development has substantially influenced the pace and extent of urbanization. Shanghai's urban economy slightly surpasses that of neighboring cities and has developed at a faster rate over the past 30 years. Since the 1980s, Shanghai's local economy has grown rapidly, with the GDP soaring from CNY 466.75 trillion in 1985 to CNY 3870.58 trillion in 2020. As depicted in Figure 9b, the urban area is linearly correlated with economic development, boasting an R^2 of 0.95; the correlation coefficient between the two is 0.976, indicating a highly significant positive correlation. In contrast, the relationship between UEA and GDP is not significant. The results suggest a more pronounced corre-

lation between Shanghai's urbanization and economic development. This implies that a higher economic level leads to a larger city size, and the agglomeration effect becomes more apparent.

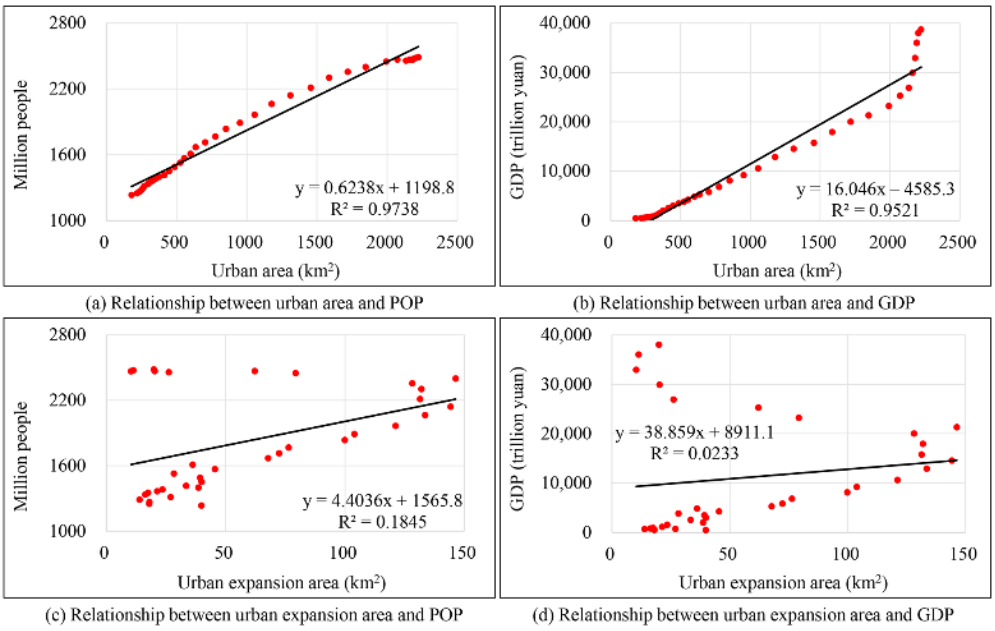

Figure 9. Urban expansion in Shanghai in relation to economic and demographic trends.

4.4.2. The Effect of Transport Network on Urban Expansion

UEAs and transport construction are mutually reinforcing processes. To analyze this relationship, we created buffers of different widths for each transport road network and extracted the area of urban expansion within each buffer. The statistics reveal that the most substantial urban expansion occurred within 0.3 km of all transport facilities and was concentrated in the period between 2005 and 2010 (Table 4 and Figure 10). The expansion area within each time period is relatively evenly distributed for areas closer to the metro.

Table 4. The relationship between UEAs and transportation.

Transportation	UEA 1985–2020 (km^2)				
	0.0–0.3 km	**0.3–0.6 km**	**0.6–0.9 km**	**0.9–1.2 km**	**1.2–1.5 km**
Primary roads	679.78	538.00	419.91	304.79	208.91
Highways	283.16	255.82	242.89	224.64	204.04
Railways	139.15	106.54	100.22	92.46	84.85
Subways	239.87	213.69	190.90	173.34	160.13

Table 4 displays the UEA at varying distances from different types of roads. The 0.0–0.3 km interval from the primary road has the most substantial UEA, totaling 679.78 km^2. As the distance from the primary road to the buffer zone increases, the UEA decreases. For railways, there is only an urban expansion of 139.15 km^2 within the 0.0–0.3 km buffers. Overall, the UEA within the buffers decreases as the distance from the transport line increases. These findings indicate that Shanghai's urban expansion relies heavily on transport development. From 1985 to 2020, major transport routes were the lifeline of Shanghai's socioeconomic development, and transport construction became the backbone and framework of the urban expansion.

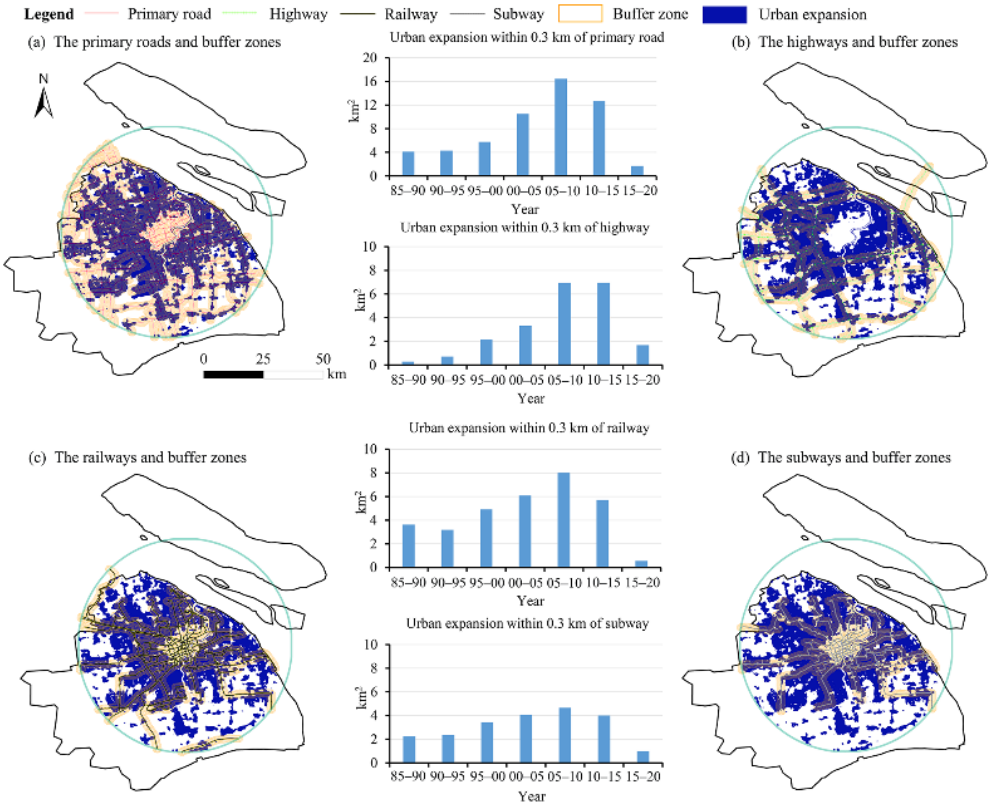

Figure 10. Urban expansion in Shanghai within 0.3 km from the roads.

4.4.3. Quantifying Driver Contribution of Urban Expansion

We quantified the impact of each driving factor on the urban expansion of Shanghai over the past 35 years by constructing a GAM. The GAM shows a decrease in Akaike information criterion (AIC) when more factors are included in the models (Table 5). These infrastructure factors explained more than 19% of the accumulative deviance explained (ADE) for urban expansion when all six factors were included in the GAM. The *p*-value of 0.254 when D_{rail} is included in the model indicates that the effect of this factor on urban expansion is not statistically significant. However, the inclusion of this driver in the GAM model reduces the AIC value from 5249.177 to 5247.854, indicating an improvement in the model fit. The GAM incorporates the other five drivers (D_{city}, D_{pri}, D_{high}, D_{dis}, and D_{sub}) sequentially with *p*-values below 0.05 and the first four factors with *p*-values below 0.001, thus making them statistically significant for urban expansion. As the factors were added in sequence, the AIC values gradually decreased, resulting in a better-performing GAM. The D_{city} has the greatest impact on urban expansion during 1985–2020, as it has the highest explanatory bias of 16.43%. The D_{rail} contributed the least to urban expansion, and the remaining factors contributed in descending order of explained deviance.

Table 5. Statistics of GAM in relationship of urban expansion and infrastructure.

Variable	GAM (1985–2020)					
	Residual Deviance	**Deviance Explained**	**ADE (%)**	**AIC**	***p*-Value**	**Rank**
Null	1054.409			6130.017		
$+D_{city}$	881.2205	173.1885	16.43	5387.458	<0.001	1
$+D_{pri}$	864.2398	16.9807	18.04	5307.373	<0.001	2
$+D_{high}$	855.3613	8.8785	18.88	5270.959	<0.001	3
$+D_{dis}$	850.8679	4.4934	19.30	5250.595	<0.001	4
$+D_{sub}$	848.2171	2.6508	19.56	5249.177	<0.05	5
$+D_{rail}$	847.8935	0.3236	19.59	5247.854	0.254	6

5. Discussion

Our study provides a comprehensive exploration of Shanghai's urban expansion from 1985 to 2035, examining key characteristics, spatial variations, expansion hotspots, and landscape dynamics. Both historically and predictively, the process of urban expansion in Shanghai has demonstrated substantial temporal and spatial heterogeneity. In the early stages, urban expansion was predominantly concentrated in the north, while later stages saw development mainly in the east and south, with the most common expansion type being peripheral. Over time, the expansion hotspots have continuously shifted outward, resulting in substantial alterations to Shanghai's landscape pattern over a span of 50 years. Moreover, population policies, economic interventions, and infrastructure development have played a pivotal role in shaping Shanghai's urban expansion. Our findings offer valuable insights into the nature of Shanghai's urban growth, contributing a scientific foundation for sustainable urban development strategies [42,54].

Our projection of urban expansion over the next 15 years reveals that the built-up area boundary of the Shanghai metropolitan region continues to expand. Urban land use persists in growing over the study period, maintaining a state of high-intensity expansion [55]. The construction land density exhibits a circular distribution, diminishing from the city center outwards, indicating a trend towards a more compact urban structure. Additionally, with a comprehensive time series spanning half a century and an unbroken time interval of one year, we observe that Shanghai's urban expansion pattern aligns closely with its developmental stage. Specifically, Shanghai has transitioned through three distinctive phases: a period of rapid expansion, a period of slow expansion, and a period of expansion stagnation. By accurately identifying historical urban expansion trends and future urban development trajectories, we can equip decision makers with a clearer understanding of the potential ecological land loss, increased water resource demands, and heightened environmental concerns associated with infrastructure growth such as the expansion of road networks. This knowledge base can inform future urban planning strategies, encouraging the integration of ecological planning, a focus on sustainable resource use, and the promotion of low-carbon transportation options.

Urban expansion refers to the evolutionary process of increasing built-up areas and outward growth, driven by the combined effects of economic development, population growth, and accelerated urbanization. Prior research has typically investigated the spatial and temporal dynamics of urban expansion using data sources such as nighttime lighting data, land use data, and socioeconomic statistics. These studies often utilize GIS spatial analysis methods and select metrics like urban expansion counts and landscape metrics [56,57]. Spatial autoregressions, the geographical weighted regression model, and generalized additive models are frequently employed by researchers to scrutinize the driving mechanisms of urban expansion [58,59]. However, there exists a gap in the literature regarding long time-series studies on urban expansion and its driving mechanisms in metropolitan areas at successive points in time, both retrospectively and prospectively.

The landscape metrics reflect land use decisions at various stages in the evolution of Shanghai's development policies [60,61]. Fluctuations in SHAPE_MN and PAFRAC suggest a rapid growth of new urban cells. Concurrently, the increase in PLAND and LPI, coupled with the decrease in ED and LSI, indicate that urban expansion is predominantly due to initial urban spread rather than the addition of new urban patches. Therefore, landscape metrics effectively identify the pattern of urban expansion in Shanghai. Additionally, the analysis of the urban expansion process, as revealed through the recognition of landscape changes, affirms that Shanghai's urban expansion mechanism aligns with the urban growth stage theory.

As Shanghai's economy flourishes, the city's central district is experiencing expansive growth marked by a swift development of infrastructure, real estate, and tertiary industries as well as the surrounding areas [62]. Concurrently, Shanghai's population has been on a steady incline, largely attributed to the influx of a transient population drawn by the city's dynamic economic growth. Additionally, as living standards continue to rise,

people's expectations for housing quality have heightened, thereby hastening the pace of property development. Shanghai's comprehensive transport network, encompassing primary roads, highways, railways, and subways, has substantially facilitated the city's expansion, propelling the increase in urban area. In sum, Shanghai's city center, with its robust economy, burgeoning population, and efficient transport network, exerts a strong radiating effect on its surrounding areas [63,64].

Our study reveals that Shanghai's urban land area continues to expand and the landscape pattern remains unstable, as evident in both the observed urban pattern from 1985 to 2020 and the projected urban pattern from 2021 to 2035. To promote high-quality development of Shanghai's land space and the harmonious development of the human–land relationship, the intensity of urban expansion and the pattern of urban agglomerations need to be meticulously managed. In light of the analysis results concerning the driving mechanism, there should be an enhancement in the synergy between Shanghai's urban expansion and its population and economic growth. Moreover, the urban development boundary should be closely interlinked with both the population and economic factors. Future work is required to evaluate the carrying capacity of Shanghai's resources and environment and to strike a balance between urban land quality and ecological and environmental protection.

6. Conclusions

In this study, we extracted the built-up area of Shanghai for the period 1985–2020 based on impervious surface products. We also simulated the future urban pattern for 2021–2035 using the CA model with the actual land pattern in 2020 as the input layer. This led to an investigation of the spatial and temporal evolution and drivers of urban expansion in the Shanghai metropolitan area over a 50-year period. Our methodology incorporated metrics such as UEA, UES, urban expansion intensity, centroid shift models, and landscape metrics. Through correlation analysis, GIS spatial analysis, and the generalized additive model, we combined remote sensing, GIS, and statistical methods to realize a spatiotemporal pattern analysis and quantification of the impacts of the drivers of urban expansion in metropolitan areas.

This analysis of urban expansion features, expansion quality, and driving mechanisms at successive points in time on a metropolitan scale, encompassing a longer time series, contributes to a comprehensive understanding of the mechanisms of urban land expansion in metropolitan areas. As urban expansion encompasses a complex system integrating social, economic, and ecological development factors, this study provides an exploratory analysis of the features and anthropogenic influences of urban expansion in metropolitan areas from a macroscopic perspective. However, it does not delve into the combined impact of the driving factors at a deeper level.

Future studies are set to further explore the natural factors influencing urban expansion in metropolitan areas and identify the mechanisms of urban land expansion. This will provide targeted reference information for metropolitan spatial planning, contributing to more informed and sustainable urban development strategies.

Author Contributions: Y.F. conceived the idea, drew the flow chart, and revised the manuscript. C.G. performed the experiments, analyzed the results, and wrote the first draft. All authors participated in the analysis of the results as well as writing and proofreading the manuscript. All authors have read and agreed to the published version of the manuscript.

Funding: Supported by the National Natural Science Foundation of China (42071371).

Data Availability Statement: The datasets are freely available at: https://figshare.com/s/348c5780449c90fa85d7.

Acknowledgments: The authors would like to thank the editors and anonymous reviewers for their constructive comments and suggestions.

Conflicts of Interest: The authors declare no conflict of interest.

References

1. Seto, K.C.; Güneralp, B.; Hutyra, L.R. Global forecasts of urban expansion to 2030 and direct impacts on biodiversity and carbon pools. *Proc. Natl. Acad. Sci. USA* **2012**, *109*, 16083–16088. [CrossRef]
2. Zhou, L.; Dang, X.; Sun, Q.; Wang, S. Multi-scenario simulation of urban land change in Shanghai by random forest and CA-Markov model. *Sustain. Cities Soc.* **2020**, *55*, 102045. [CrossRef]
3. Talkhabi, H.; Ghalehteimouri, K.J.; Mehranjani, M.S.; Zanganeh, A.; Karami, T. Spatial and temporal population change in the Tehran Metropolitan Region and its consequences on urban decline and sprawl. *Ecol. Inform.* **2022**, *70*, 101731. [CrossRef]
4. Liu, J.; Kuang, W.; Zhang, Z.; Xu, X.; Qin, Y.; Ning, J.; Zhou, W.; Zhang, S.; Li, R.; Yan, C.; et al. Spatiotemporal characteristics, patterns, and causes of land-use changes in China since the late 1980s. *J. Geogr. Sci.* **2014**, *24*, 195–210. [CrossRef]
5. Wei, Y.D.; Ye, X. Urbanization, urban land expansion and environmental change in China. *Stoch. Environ. Res. Risk Assess.* **2014**, *28*, 757–765. [CrossRef]
6. Li, J.; Lei, J.; Li, S.; Yang, Z.; Tong, Y.; Zhang, S.; Duan, Z. Spatiotemporal analysis of the relationship between urbanization and the eco-environment in the Kashgar metropolitan area, China. *Ecol. Indic.* **2022**, *135*, 108524. [CrossRef]
7. Long, H.; Tang, G.; Li, X.; Heilig, G.K. Socio-economic driving forces of land-use change in Kunshan, the Yangtze River Delta economic area of China. *J. Environ. Manag.* **2007**, *83*, 351–364. [CrossRef]
8. Shen, S.; Yue, P.; Fan, C. Quantitative assessment of land use dynamic variation using remote sensing data and landscape pattern in the Yangtze River Delta, China. *Sustain. Comput. Inform. Syst.* **2019**, *23*, 111–119. [CrossRef]
9. Liu, J.; Zhan, J.; Deng, X. Spatio-temporal patterns and driving forces of urban land expansion in China during the economic reform era. *AMBIO A J. Hum. Environ.* **2005**, *34*, 450–455. [CrossRef]
10. Doe, B.; Amoako, C.; Adamtey, R. Spatial expansion and patterns of land use/land cover changes around Accra, Ghana—Emerging insights from Awutu Senya East Municipal Area. *Land Use Policy* **2021**, *112*, 105796. [CrossRef]
11. Chen, Z.; Yu, B.; Song, W.; Liu, H.; Wu, Q.; Shi, K.; Wu, J. A new approach for detecting urban centers and their spatial structure with nighttime light remote sensing. *IEEE Trans. Geosci. Remote Sens.* **2017**, *55*, 6305–6319. [CrossRef]
12. Angel, S.; Parent, J.; Civco, D.L.; Blei, A.; Potere, D. The dimensions of global urban expansion: Estimates and projections for all countries, 2000–2050. *Prog. Plan.* **2011**, *75*, 53–107. [CrossRef]
13. Sejati, A.W.; Buchori, I.; Rudiarto, I. The spatio-temporal trends of urban growth and surface urban heat islands over two decades in the Semarang Metropolitan Region. *Sustain. Cities Soc.* **2019**, *46*, 101432. [CrossRef]
14. He, C.; Okada, N.; Zhang, Q.; Shi, P.; Zhang, J. Modeling urban expansion scenarios by coupling cellular automata model and system dynamic model in Beijing, China. *Appl. Geogr.* **2006**, *26*, 323–345. [CrossRef]
15. Du, X.; Huang, Z. Ecological and environmental effects of land use change in rapid urbanization: The case of hangzhou, China. *Ecol. Indic.* **2017**, *81*, 243–251. [CrossRef]
16. Hegazy, I.R.; Kaloop, M.R. Monitoring urban growth and land use change detection with GIS and remote sensing techniques in Daqahlia governorate Egypt. *Int. J. Sustain. Built Environ.* **2015**, *4*, 117–124. [CrossRef]
17. Mahmoud, H.; Alfons, R.; Reffat, R.M. Analysis of the driving forces of urban expansion in luxor city by remote sensing monitoring. *Int. J. Integr. Eng.* **2019**, *11*, 296–307. [CrossRef]
18. Gao, C.; Feng, Y.; Tong, X.; Jin, Y.; Liu, S.; Wu, P.; Ye, Z.; Gu, C. Modeling urban encroachment on ecological land using cellular automata and cross-entropy optimization rules. *Sci. Total Environ.* **2020**, *744*, 140996. [CrossRef]
19. Hong, W.; Jiang, R.; Yang, C.; Zhang, F.; Su, M.; Liao, Q. Establishing an ecological vulnerability assessment indicator system for spatial recognition and management of ecologically vulnerable areas in highly urbanized regions: A case study of Shenzhen, China. *Ecol. Indic.* **2016**, *69*, 540–547. [CrossRef]
20. Banzhaf, E.; Grescho, V.; Kindler, A. Monitoring urban to peri-urban development with integrated remote sensing and GIS information: A Leipzig, Germany case study. *Int. J. Remote Sens.* **2009**, *30*, 1675–1696. [CrossRef]
21. Odindi, J.; Mhangara, P.; Kakembo, V. Remote sensing land-cover change in Port Elizabeth during South Africa's democratic transition. *South Afr. J. Sci.* **2012**, *108*, 7. [CrossRef]
22. Li, C.; Chen, F.; Wang, N.; Yu, B.; Wang, L. SDGSAT-1 nighttime light data improve village-scale built-up delineation. *Remote Sens. Environ.* **2023**, *297*, 113764. [CrossRef]
23. Aguilera, F.; Valenzuela, L.M.; Botequilha-Leitão, A. Landscape metrics in the analysis of urban land use patterns: A case study in a Spanish metropolitan area. *Landsc. Urban Plan.* **2011**, *99*, 226–238. [CrossRef]
24. Sharma, K. Urbanization induced land use-land cover changes in the Manipur valley and surrounding hills: A landscape metrics approach. In *Environmental Change in the Himalayan Region*; Springer: Berlin/Heidelberg, Germany, 2019; pp. 137–155.
25. Jiao, L.; Gong, C.; Xu, G.; Dong, T.; Zhang, B.; Li, Z. Urban expansion dynamics and urban forms in three metropolitan areas—Tokyo, New York, and Shanghai. *Prog. Geogr.* **2019**, *38*, 675–685.
26. Yu, S.; Zhang, Z.; Liu, F.; Wang, X.; Hu, S. Urban expansion in the megacity since 1970s: A case study in Mumbai. *Geocarto Int.* **2021**, *36*, 603–621. [CrossRef]
27. Akintunde, J.; Adzandeh, E.; Fabiyi, O. Spatio-temporal pattern of urban growth in Jos Metropolis, Nigeria. *Remote Sens. Appl. Soc. Environ.* **2016**, *4*, 44–54. [CrossRef]
28. Zhao, M.; Cai, H.; Qiao, Z.; Xu, X. Influence of urban expansion on the urban heat island effect in Shanghai. *Int. J. Geogr. Inf. Sci.* **2016**, *30*, 2421–2441. [CrossRef]

29. Shi, G.; Jiang, N.; Yao, L. Land use and cover change during the rapid economic growth period from 1990 to 2010: A case study of Shanghai. *Sustainability* **2018**, *10*, 426. [CrossRef]
30. You, H. Quantifying the coordinated degree of urbanization in Shanghai, China. *Qual. Quant.* **2015**, *50*, 1273–1283. [CrossRef]
31. Cui, X.; Wang, X. Urban land use change and its effect on social metabolism: An empirical study in Shanghai. *Habitat Int.* **2015**, *49*, 251–259. [CrossRef]
32. Cui, L.; Shi, J. Urbanization and its environmental effects in Shanghai, China. *Urban Clim.* **2012**, *2*, 1–15. [CrossRef]
33. He, J.; Wang, S.; Liu, Y.; Ma, H.; Liu, Q. Examining the relationship between urbanization and the eco-environment using a coupling analysis: Case study of Shanghai, China. *Ecol. Indic.* **2017**, *77*, 185–193. [CrossRef]
34. Feng, Y.; Liu, Y.; Tong, X. Spatiotemporal variation of landscape patterns and their spatial determinants in Shanghai, China. *Ecol. Indic.* **2018**, *87*, 22–32. [CrossRef]
35. Li, J.; Li, C.; Zhu, F.; Song, C.; Wu, J. Spatiotemporal pattern of urbanization in Shanghai, China between 1989 and 2005. *Landsc. Ecol.* **2013**, *28*, 1545–1565. [CrossRef]
36. Feng, Y.; Tong, X. A new cellular automata framework of urban growth modeling by incorporating statistical and heuristic methods. *Int. J. Geogr. Inf. Sci.* **2019**, *34*, 74–97. [CrossRef]
37. Wu, F.; Webster, C.J. Simulation of land development through the integration of cellular automata and multicriteria evaluation. *Environ. Plan. B Plan. Des.* **1998**, *25*, 103–126. [CrossRef]
38. Wang, S.; Liu, J.; Zhang, Z. Spatial pattern change of land use in China in recent 10 years. *Acta Geogr. Sin.* **2002**, *57*, 523–530.
39. Li, F.; Zhou, T. Effects of urban form on air quality in China: An analysis based on the spatial autoregressive model. *Cities* **2019**, *89*, 130–140. [CrossRef]
40. Xu, X.; Min, X. Quantifying spatiotemporal patterns of urban expansion in China using remote sensing data. *Cities* **2013**, *35*, 104–113. [CrossRef]
41. Liu, M.; Xu, Y.; Hu, Y.; Li, C.; Sun, F.; Chen, T. A Century of the evolution of the urban area in Shenyang, China. *PLoS ONE* **2014**, *9*, e98847. [CrossRef]
42. Xu, C.; Liu, M.; Zhang, C.; An, S.; Yu, W.; Chen, J.M. The spatiotemporal dynamics of rapid urban growth in the Nanjing metropolitan region of China. *Landsc. Ecol.* **2007**, *22*, 925–937. [CrossRef]
43. Zhang, Z.; Li, N.; Wang, X.; Liu, F.; Yang, L. A comparative study of urban expansion in Beijing, Tianjin and Tangshan from the 1970s to 2013. *Remote Sens.* **2016**, *8*, 496. [CrossRef]
44. Herold, M.; Scepan, J.; Clarke, K.C. The use of remote sensing and landscape metrics to describe structures and changes in urban land uses. *Environ. Plan. A Econ. Space* **2002**, *34*, 1443–1458. [CrossRef]
45. McGarigal, K. *FRAGSTATS: Spatial Pattern Analysis Program for Quantifying Landscape Structure*; US Department of Agriculture, Forest Service, Pacific Northwest Research Station: Portland, OR, USA, 1995; Volume 351.
46. Gogtay, N.J.; Thatte, U.M. Principles of correlation analysis. *J. Assoc. Physicians India* **2017**, *65*, 78–81. [PubMed]
47. Cohen, I.; Huang, Y.; Chen, J.; Benesty, J. Pearson Correlation Coefficient. In *Noise Reduction in Speech Processing*; Springer: Berlin/Heidelberg, Germany, 2009; pp. 1–4.
48. Dong, P.; Yang, C.; Rui, X.; Zhang, L.; Cheng, Q. An effective buffer generation method in GIS. In Proceedings of the IGARSS 2003. 2003 IEEE International Geoscience and Remote Sensing Symposium; Proceedings (IEEE Cat. No. 03CH37477), Toulouse, France, 21–25 July 2003; IEEE: New York, NY, USA; Volume 6, pp. 3706–3708.
49. Bakhshi, A.K.; Ahmed, M.M. Real-time crash prediction for a long low-traffic volume corridor using corrected-impurity importance and semi-parametric generalized additive model. *J. Transp. Saf. Secur.* **2021**, *14*, 1165–1200. [CrossRef]
50. Zhang, K.; Wang, R.; Shen, C.; Da, L. Temporal and spatial characteristics of the urban heat island during rapid urbanization in Shanghai, China. *Environ. Monit. Assess.* **2010**, *169*, 101–112. [CrossRef]
51. Chang, X.; Huang, X.; Jiang, X.; Xiao, R. Impacts of Transportation Networks on the Landscape Patterns—A Case Study of Shanghai. *Remote Sens.* **2022**, *14*, 4060. [CrossRef]
52. Gong, P.; Li, X.; Zhang, W. 40-Year (1978–2017) human settlement changes in China reflected by impervious surfaces from satellite remote sensing. *Sci. Bull.* **2019**, *64*, 756–763. [CrossRef] [PubMed]
53. Zhang, X.; Liu, L.Y.; Wu, C.S.; Chen, X.D.; Gao, Y.; Xie, S.; Zhang, B. Development of a global 30 m impervious surface map using multisource and multitemporal remote sensing datasets with the Google Earth Engine platform. *Earth Syst. Sci. Data* **2020**, *12*, 1625–1648. [CrossRef]
54. Tian, S.; Wu, W.; Shen, Z.; Wang, J.; Liu, X.; Li, L.; Li, X.; Liu, X.; Chen, H. A cross-scale study on the relationship between urban expansion and ecosystem services in China. *J. Environ. Manag.* **2022**, *319*, 115774. [CrossRef]
55. Shi, L.; Shao, G.; Cui, S.; Li, X.; Lin, T.; Yin, K.; Zhao, J. Urban three-dimensional expansion and its driving forces—A case study of Shanghai, China. *Chin. Geogr. Sci.* **2009**, *19*, 291–298. [CrossRef]
56. Yue, W.; Fan, P.; Wei, Y.D.; Qi, J. Economic development, urban expansion, and sustainable development in Shanghai. *Stoch. Environ. Res. Risk Assess.* **2014**, *28*, 783–799. [CrossRef]
57. Zhang, Q.; Ban, Y.; Liu, J.; Hu, Y. Simulation and analysis of urban growth scenarios for the Greater Shanghai Area, China. *Comput. Environ. Urban Syst.* **2011**, *35*, 126–139. [CrossRef]
58. Zhao, P. Sustainable urban expansion and transportation in a growing megacity: Consequences of urban sprawl for mobility on the urban fringe of Beijing. *Habitat Int.* **2010**, *34*, 236–243. [CrossRef]

59. Wu, W.; Zhao, S.; Zhu, C.; Jiang, J. A comparative study of urban expansion in Beijing, Tianjin and Shijiazhuang over the past three decades. *Landsc. Urban Plan.* **2015**, *134*, 93–106. [CrossRef]
60. Bielsa, I.; Pons, X.; Bunce, B. Agricultural abandonment in the North Eastern Iberian Peninsula: The use of basic landscape metrics to support planning. *J. Environ. Plan. Manag.* **2005**, *48*, 85–102. [CrossRef]
61. Mohammadreza, E.L.M.İ.; Rouhani, A.; Keshavarz, E. Landscape metrics for urbanization and urban land-use change monitoring from remote sensing images: A case of Shiraz Metropolis, Iran. *Int. J. Earth Sci. Knowl. Appl.* **2022**, *4*, 43–50.
62. Pucher, J.; Peng, Z.R.; Mittal, N.; Zhu, Y.; Korattyswaroopam, N. Urban transport trends and policies in China and India: Impacts of rapid economic growth. *Transp. Rev.* **2007**, *27*, 379–410. [CrossRef]
63. Han, J.; Hayashi, Y.; Cao, X.; Imura, H. Application of an integrated system dynamics and cellular automata model for urban growth assessment: A case study of Shanghai, China. *Landsc. Urban Plan.* **2009**, *91*, 133–141. [CrossRef]
64. Kumar, A.; Verma, S.K. Design and development of e-smart robotics-based underground solid waste storage and transportation system. *J. Clean. Prod.* **2022**, *343*, 130987. [CrossRef]